

1 **Large-scale variation in wave attenuation of oyster reef living shorelines and the influence
2 of inundation duration**

3 Rebecca L. Morris¹, Megan K. La Peyre², Bret M. Webb³, Danielle A. Marshall⁴, Donna M.
4 Bilkovic⁵, Just Cebrian⁶, Giovanna McClenachan^{7,8}, Kelly M. Kibler⁹, Linda J. Walters⁷, David
5 Bushek¹⁰, Eric L. Sparks^{11,12}, Nigel A. Temple¹¹, Joshua Moody¹³, Kory Angstadt⁵, Joshua
6 Goff¹⁴, Maura Boswell¹⁵, Paul Sacks⁷, and Stephen E. Swearer¹

7

8 ¹National Centre for Coasts and Climate, School of BioSciences, The University of Melbourne,
9 VIC 3010, Australia; ²U.S. Geological Survey, Louisiana Cooperative Fish and Wildlife
10 Research Unit, School of Renewable Natural Resources, Louisiana State University Agricultural
11 Center, Baton Rouge, LA 70803, USA; ³Department of Civil, Coastal & Environmental
12 Engineering, University of South Alabama, Mobile, AL 36688, USA; ⁴School of Renewable
13 Natural Resources, Louisiana State University Agricultural Center, Baton Rouge, LA 70803,
14 USA; ⁵Virginia Institute of Marine Science, William & Mary, Gloucester Point, VA 23062,
15 USA; ⁶Northern Gulf Institute, Mississippi State University, Stennis Space Center, MS 39529,
16 USA; ⁷Department of Biology and National Center for Integrated Coastal Research, University
17 of Central Florida, Orlando, FL 32816, USA; ⁸Department of Biological Sciences, Nicholls State
18 University, Thibodaux, LA 70301, USA; ⁹Department of Civil, Environmental & Construction
19 Engineering and National Center for Integrated Coastal Research, University of Central Florida,
20 Orlando, FL 32816, USA; ¹⁰Haskin Shellfish Research Laboratory, Rutgers University, Port
21 Norris, NJ 08349, USA; ¹¹Coastal Research and Extension Center, Mississippi State University,
22 Biloxi, MS 39532, USA; ¹²Mississippi-Alabama Sea Grant Consortium, Ocean Springs, MS
23 39564, USA; ¹³Partnership for Delaware Estuary, Wilmington, DE 19801, USA; ¹⁴Dauphin

24 Island Sea Lab, Dauphin Island, AL 36528, USA; ¹⁵Department of Civil and Environmental
25 Engineering, Old Dominion University, Norfolk, VA 23529, USA.

26

27 Corresponding Author:

28 Rebecca Morris, Email rebecca.morris@unimelb.edu.au, Tel. +61 4 2339 2882

29

30

31 Running headline: Oyster reefs and coastal defence

32

33

34

35

36

37

38

39

40

41

42

43

44

45 **Abstract**

46 One of the paramount goals of oyster reef living shorelines is to achieve sustained and adaptive
47 coastal protection, which requires meeting ecological (i.e., develop a self-sustaining oyster
48 population) and engineering (i.e., provide coastal defence) targets. In a large-scale comparison
49 along the Atlantic and Gulf coasts of the United States, the efficacy of various designs of oyster
50 reef living shorelines at providing wave attenuation was evaluated accounting for the ecological
51 limitations of oysters with regards to inundation duration. A critical threshold for intertidal oyster
52 reef establishment is 50% inundation duration. Living shorelines that spent less than half of the
53 time (< 50%) inundated were not considered suitable habitat for oysters, however, were effective
54 at wave attenuation (68% reduction in wave height). Reefs that experienced > 50% inundation
55 were considered suitable habitat for oysters, but wave attenuation was similar to controls (no
56 reef; ~5% reduction in wave height). Many of the oyster reef living shoreline approaches
57 therefore failed to optimize the ecological and engineering goals. In both inundation regimes,
58 wave transmission decreased with an increasing freeboard (difference between reef crest
59 elevation and water level), supporting its importance in the wave attenuation capacity of oyster
60 reef living shorelines. However, given that the reef crest elevation (and thus freeboard) should be
61 determined by the inundation duration requirements of oysters, research needs to be re-focused
62 on understanding the implications of other reef parameters (e.g. width) for optimising wave
63 attenuation. A broader understanding of the reef characteristics and seascape contexts that result
64 in effective coastal defence by oyster reefs is needed to inform appropriate design and
65 implementation of oyster-based living shorelines globally.

66 Keywords: coastal management; coastal erosion; nature-based coastal defence; shoreline
67 protection; wave transmission

68 **Introduction**

69 Oyster reefs are highly valued as a fishery resource and as biogenic habitat for a diverse suite of
70 marine species (Grabowski et al. 2012, Cohen and Humphries 2017). Their ecological and socio-
71 economic worth has driven extensive oyster reef restoration, in response to widespread declines
72 in oyster populations (85% functionally extinct; Beck et al. 2011). Recently, there has been
73 increased interest in constructing or restoring oyster reefs for living shoreline applications to
74 stem erosion (Piazza et al. 2005; Bilkovic et al. 2016). Living shorelines are engineered
75 structures primarily composed of natural materials that can be used as an alternative to other
76 “harder” engineered structures, such as seawalls and rock revetments, which are environmentally
77 (Bulleri and Chapman 2010) and economically (Hinkel et al. 2014) costly. Oyster reefs can alter
78 hydrodynamic conditions in estuarine systems through increasing bed friction (Wright et al.
79 1990, Whitman and Reidenbach 2012, Styles 2015, Kitsikoudis et al. 2020), facilitating wave
80 attenuation (Manis et al. 2015) and accreting sediment on the leeward side of the reef (Salvador
81 de Paiva et al. 2018, Chowdhury et al. 2019). This will become particularly relevant in the future
82 as increased risk of climate change-related erosion and flooding to burgeoning human
83 populations along the coast (Young et al. 2011, Neumann et al. 2015, Meucchi et al. 2020) will
84 result in an increased need for investment in coastal protection infrastructure, and the
85 development of adaptive and sustainable approaches to shoreline protection (Morris et al. 2020).

86 Traditional coastal defence structures (e.g., seawalls, breakwaters) have usually
87 undergone extensive numerical and physical modelling to identify the important design
88 parameters and their performance under various environmental conditions (e.g. wave heights,
89 water depths). Low crested breakwaters are constructed at or below the water level (i.e.,
90 submerged), and can inform wave transmission at oyster reef living shorelines. In low crested

91 breakwaters, wave transmission is most sensitive to the depth of breakwater submergence, the
92 incident wave height, and the crest width (Seabrook and Hall, 1998; van der Meer et al. 2005).
93 Wave transmission increases with increased submergence, increased incident wave height, and
94 decreased crest width (Seabrook and Hall, 1998; van der Meer et al. 2005). Crest width becomes
95 particularly important as submergence increases, whereas freeboard (difference between reef
96 crest elevation and water level) has a larger effect when submergence is reduced (Seabrook and
97 Hall, 1998). Secondarily, the period of the incident wave, the breakwater armour dimensions (in
98 the case of a rubble mound structure), and the breakwater slope have small effects on wave
99 transmission (Seabrook and Hall 1998).

100 Similar to breakwater construction, the creation of an oyster reef living shoreline begins
101 with the placement of reef substratum such as oyster shell, pre-cast concrete structures, or
102 crushed limestone (Hernandez et al. 2018, Morris et al. 2019a) for oyster colonisation. Physical
103 modelling of the reef substrate agrees with findings from low-crested breakwaters that the
104 freeboard, crest width and incident wave height are key parameters for wave transmission (Allen
105 and Webb 2011, Webb and Allen 2015, Coghlan et al. 2016). This pattern of wave attenuation as
106 a function of water depth in relation to the crest elevation has also been confirmed in field
107 studies (Chauvin 2018, MacDonald 2018, Wiberg et al. 2018, Chowdhury et al. 2019, Zhu et al.
108 2020, Spiering et al. in revision). While this research has clearly shown that a smaller
109 submergence results in greater wave attenuation by oyster reefs, these findings do not take into
110 account oyster habitat requirements, a necessary consideration for the appropriate application of
111 oyster reef-based living shorelines.

112 Unlike static structures, the vertical reef building capacity of oysters makes them a
113 candidate for creating dynamic structures (Mitchell and Bilkovic 2019). Oyster reefs exhibit a

114 natural resilience and adaptive capacity to recover quickly from major storm events (Livingston
115 et al. 1999) and are capable of accreting at a rate necessary to maintain elevation in areas facing
116 sea-level rise (Rodriguez et al. 2014) or local subsidence (Casas et al. 2015). A key variable that
117 affects the recruitment, survival, and growth of oyster reefs is the duration of inundation (Table
118 1), which is a function of the absolute elevation of the reef and the tidal range. The lower
119 elevation threshold of intertidal oysters is commonly determined by increased biofouling,
120 predation, competition, or sedimentation in the subtidal (Fodrie et al. 2014, Solomon et al. 2014),
121 whereas the maximum elevation of oysters in the intertidal is driven by availability of filter
122 feeding time and exposure to extreme temperature stress. The optimum inundation duration,
123 therefore, is a trade-off among these limiting factors. The inundation duration has been
124 reasonably well-studied for the eastern oyster (*Crassostrea virginica*) in some locations along the
125 east coast of the United States (Table 1). This species is generally found at 60-80% inundation,
126 with lower and upper boundaries at 50% and 95% inundation, respectively (Fodrie et al. 2014;
127 Byers et al. 2015; Ridge et al. 2014, 2017; Solomon et al. 2014; Marshall and La Peyre, 2020;
128 Table 1). Thus, for intertidal oysters, constructing a reef base at an elevation that spends more
129 than 50% of the time inundated is critical for oyster establishment. Consequently, there is a
130 dichotomy between the reef elevation for optimal engineering design and habitat provisioning for
131 oysters.

132 As efforts to characterise wave attenuation by oyster reef living shorelines are growing,
133 the aim of this paper is to assess whether observed trends in oyster reef wave attenuation apply
134 across different environments and reef types using data across a large spatial scale. Further, we
135 consider wave transmission alongside the ecological limitations for oysters to characterize the
136 expected balance between effective wave attenuation and likelihood of reef persistence. Wave

137 attenuation was measured at 15 oyster reef living shoreline-control pairs in five locations (New
138 Jersey/Delaware, Virginia, Florida, Alabama and Louisiana) along the Atlantic and Gulf coasts
139 of the United States. At each location we assessed the effects of oyster reef living shorelines
140 compared to controls (no reef) on wave attenuation relative to the inundation duration of the reef.
141 It was predicted that: (1) wave transmission would be greater at oyster reefs with an inundation
142 duration of > 50% compared with < 50%; (2) for oyster reefs with an inundation duration of >
143 50%, wave attenuation would increase with width; and (3) there would be a difference in wave
144 transmission between shell-based and concrete-based oyster reefs. Furthermore, at the Virginia
145 and Florida reefs, we compared the wave height attenuation of oyster reef living shorelines to
146 rock sills and natural unrestored oyster reefs, respectively.

147

148 **Methods**

149 **Study locations**

150 The fifteen oyster reef living shoreline (hereafter, “oyster reef”)-control pairs (Fig. 1) were
151 selected to cover the diversity of techniques commonly employed, which varied within and
152 among states in terms of age, materials, and size (Table 2; Appendix S1: Table S1). The wave
153 climate in the offshore waters at each location was observed at the NDBC (National Data Buoy
154 Center) stations (Appendix S1: Fig. S1), and the wind field was observed at the closest NOAA
155 (National Oceanic and Atmospheric Administration) climate station (Appendix S1: Fig. S1) over
156 a two-year period from 2017 – 2018 and during the study period at each location (one week).
157 Wind fetch distances were calculated for each site using fetchR (Seers 2018).

158

159 *New Jersey/Delaware*

160 Study sites at Nantuxent (NJ1; 39.2848, -75.2361) and Gandy's Beach (NJ2; 39.2789, -
161 75.2430) were located on the western shore of New Jersey; the site at Mispillion (NJ3; 38.9477, -
162 75.3149) was located on the eastern shore of Delaware, in Delaware Bay (Table 2). In 2016, nine
163 shell bag oyster reefs were installed at Gandy's Beach on land owned by The Nature
164 Conservancy, and a series of Oyster Castles® were installed at Nantuxent next to Money Island
165 Marina (The Nature Conservancy 2017). These sites have high value, both economically (Money
166 Island Marina was the off-load point for the NJ commercial oyster fleet) and environmentally
167 (Gandy's Beach is a nesting site for horseshoe crabs and a feeding ground for the migrating red
168 knot). Oyster Castles® were also installed at the mouth of the Mispillion River, immediately
169 adjacent to the DuPont Nature Center (Moody et al. 2016), situated across the river from a large
170 breakwater present on the bay-side. This site is a common feeding area for red knots during their
171 spring/summer migration, is home to one of a few naturally occurring intertidal oyster reefs in
172 Delaware, and the aim was to expand the natural oyster reef to stabilize eroding saltmarsh.

173 The tides in Delaware Bay are semi-diurnal, and the mean tidal range is 1.7 m (NOAA
174 station 8535055; Table 2). In the offshore waters, the predominant wave direction is from the
175 east and south-east, with an average significant wave height of 1.05 m from this direction in the
176 period 2017 – 2018, and 0.83 m during the study period (Appendix 1: Fig. S2). The predominant
177 wind direction is from the west, where the greatest wind speeds were recorded during the study
178 period (Appendix 1: Fig. S3). This corresponded to the direction with the largest fetch distances
179 at NJ1 and NJ2 (Appendix S1: Table S1). During the deployment at NJ3, wind speeds were low
180 ($< 4 \text{ ms}^{-1}$) from the east and south.

181

182 *Virginia*

183 Diggs (VA3; 37.4473, -76.2605) was located in Chesapeake Bay and Laws (VA1;
184 36.8973, -76.2721) and Captain Sinclair (VA2; 37.3245, -76.4275) were located in two sub-
185 estuaries of Chesapeake Bay, the Lafayette River and Mobjack Bay, respectively (Table 2). The
186 oyster reefs were constructed in 2016 – 2017 as erosion control for private waterfront properties
187 and were made of Ready Reef, Oyster Castles® and bagged shell for Diggs, Laws, and Captain
188 Sinclair, respectively. At all of the sites, there was also a section of shoreline protected by a rock
189 sill with saltmarsh.

190 The tides in Chesapeake Bay are semi-diurnal and the mean tidal range is 0.7 m (NOAA
191 station 8637689; Table 2). In the offshore waters, the predominant wave direction is from the
192 east and south-east, with an average significant wave height of 0.93 m from this direction in the
193 period 2017 – 2018, and 0.68 m during the study period (Appendix 1: Fig. S2). A southerly wind
194 was predominant during the study period (Appendix 1: Fig. S3), which corresponded to the
195 direction of the highest fetch at VA1 and VA2 (Appendix S1: Table S1). Although, the strongest
196 wind (above 8 m s^{-1}) was recorded from the north during the study, the direction with the largest
197 fetch at VA3 (Appendix S1: Fig. S3; Table S1).

198

199 *Florida*

200 Florida sites were located on the east coast of Central Florida in Mosquito Lagoon, which
201 encompasses the northernmost section of the Indian River Lagoon system (Table 2). The tides
202 are semi-diurnal and the mean tidal range is 0.3 m (NOAA station 8721222; Table 2). The Indian
203 River Lagoon System is long (195 km), shallow (1-3 m) and narrow (2-4 km), making it
204 extremely fetch-limited (Appendix S1: Table S1) and only persistent south-east or north-west

205 winds tend to cause flooding and erosion (Colvin et al. 2018). During the study the predominant
206 winds were from the south and southwest (Appendix 1: Fig. S3). In the offshore waters, the
207 predominant wave direction is from the east and northeast, with an average significant wave
208 height of 1.18 m from this direction in the period 2017 – 2018, and 0.48 m during the study
209 period (Appendix 1: Fig. S2).

210 The oyster reefs Mosquito (FL1; 25.9589, -80.8746), Hallmark (FL2; 28.9684, -80.8803)
211 and Pufferfish (FL3; 28.9699, -80.8818) were oyster reef restoration projects constructed in
212 2010, 2017 and 2016, respectively using the oyster mat method (oyster shells attached to
213 aquaculture grade mesh; www.restoreourshores.org). The oyster reefs were restored on the
214 historic footprint of degraded natural reefs, and at all sites there were natural unrestored oyster
215 reefs adjacent to the oyster reef living shoreline.

216

217 *Alabama*

218 Alabama study sites were located in Portersville Bay; Northeastern Point aux Pines (AL1;
219 30.3881, -88.2943) was on the north-eastern portion of a peninsula in the bay (Sharma et al.
220 2016), while Coffee Island 1 and 2 (AL2, AL3; 30.3428, -88.2552) were on the eastern shoreline
221 of Coffee Island (or Isle aux Herbes) (Table 2). The Point aux Pines reef was constructed in 2009
222 comprising three 25 m units of loose shell. The Coffee Island reefs, constructed in 2010, were
223 made of experimental units of bagged shell, ReefBLKSM and Reef BallTM, the latter two were
224 used in this study (Heck et al. 2012).

225 The tides in Portersville Bay are diurnal and the mean tidal range is 0.4 m (NOAA station
226 8735180; Table 2). In the offshore waters, the predominant wave direction is from the south and
227 south-east, with an average significant wave height of 0.89 m from this direction in the period

228 2017 – 2018, and 0.57 m during the study period (Appendix 1: Fig. S2). The most persistent
229 winds during the study were from the east and south-east (Appendix 1: Fig. S3), which also
230 corresponded to the direction of greatest fetch at these sites (i.e., south and east; Appendix S1:
231 Table S1). The small percentage of wind events $> 10 \text{ m s}^{-1}$ from the south/east direction were not
232 captured in this study, which likely result in the greatest wave events at these sites.

233

234 *Louisiana*

235 The sites were in the Biloxi Marsh estuary in Eloi Bay (LA1, LA2; 29.7760, -89.4071)
236 and Lake Athanasio (LA3; 29.7459, -88.4688) in southeastern Louisiana (Table 2). This location
237 has diurnal tides with a mean tidal range of 0.4 m (NOAA station 8761305; Table 2). In Eloi
238 Bay, the living shoreline was constructed by the Coastal Protection and Restoration Authority of
239 Louisiana (CPRA) in 2016 to reduce wave energy in order to minimize adjacent marsh erosion
240 and provide a platform for oysters to grow on. A coastal engineering analysis based on wave
241 attenuation and stability was used to determine the final living shoreline design, which
242 incorporated multiple bioengineered designs, including Wave Attenuation Devices (WAD[®]) and
243 ShoreJAXTM, which were used in this study (Carter et al. 2016). At Lake Athanasio an
244 OysterbreakTM shoreline protection reef was built by The Nature Conservancy in 2011. Wave
245 data for the period 2017 – 2018 were not available for these sites, however, modelling by CHE
246 (2014) showed that the annual average wave height at the CPRA reefs between 1980 - 2012 was
247 0.43 m (Appendix 1: Fig. S2). Relatively low wind speeds ($< 6 \text{ ms}^{-1}$) were recorded
248 predominantly from the northwest and west during the study. The largest fetch distances are
249 from the south and east at the sites in this location, which was the prevailing wind direction
250 during 2017 – 2018 (Appendix S1: Table S1, Fig. S2).

251

252 **Data collection**

253 Wave loggers (RBR[®] *solo* D wave; hereafter RBRs) were deployed for 48 hours (36 hrs for NJ2,
254 NJ3 and FL2 due to tide times and distance to travel between sites) at each reef, rotated over 5
255 weeks in June - July 2018. At each site four RBRs were deployed at a control (no reef) and
256 oyster reef treatment; one each placed offshore and onshore of the control or reef area (~ 2-5 m
257 from the on- and off- shore reef edge; Fig. 1b). The control was selected to be as close to the reef
258 as possible (site dependent; a minimum of ~ 10 m), yet outside the reef zone of wave influence,
259 maintaining similar shoreline characteristics (e.g. vegetation, substrate type), orientation and
260 fetch. The RBRs were attached with cable ties to a metal or PVC pole that was hammered into
261 the seabed and the transect length between the onshore and offshore RBRs at each treatment was
262 measured. The RBRs were programmed using the software Ruskin (v1.13.12; mode = wave;
263 frequency = 1 Hz; duration = 1024; burst rate = 1 hour) to collect wave data (significant wave
264 height, H_s , in metres and associated period, T , in seconds). The wave data collected is assumed to
265 be primarily wind-driven, however, boat wakes may also be important wave sources in some
266 locations (Garvis 2009) and could have contributed to the wave heights in this study.

267 At LA1 and LA2, five RBRs were deployed: two placed onshore and offshore of the
268 control and three placed around two replicate reefs (two onshore of each reef and one offshore of
269 the reefs). A different set-up was used due to the difficulty of returning to the sites over multiple
270 days to rotate the RBRs (5 RBRs were the maximum we had available). As the reefs were
271 aligned with a similar orientation along the shoreline, we assumed that the offshore wave energy
272 would be consistent between reefs. There was no significant difference between the wave heights

273 recorded at the offshore RBR for the control and reef treatments ($t_{(37)} = -1.1996$, $P > 0.05$),
274 providing further support of this assumption.

275 Ten photo-quadrats (0.09 m^2) were taken of each reef at New Jersey, Delaware, Virginia
276 and Florida and the percentage cover of oysters was calculated using 25 random points assigned
277 using the program CPCe4.1 (Kohler and Gill, 2006). The percentage cover of oysters could not
278 be quantified at Alabama or Louisiana as water levels were too high during the sampling period
279 and the water too turbid to take photo-quadrats. The size of the reef (length, width, height) and
280 distance from shoreline was either measured in the field during RBR deployment or determined
281 from aerial imagery using ArcGIS. All reefs were positioned parallel to the shore.

282 In Virginia and Florida, rock sills and natural oyster reefs were added as an additional
283 treatment to the experimental design, respectively. In Virginia, rock sills were present at all sites
284 adjacent to the oyster reef living shoreline, and two additional RBRs were positioned onshore
285 and offshore of the structure at the same time as the oyster reef and control treatments, as before.
286 Unfortunately, one RBR was lost in a storm during the last deployment in Virginia, which left
287 five for deployment in Florida. Therefore, in Florida one RBR was placed onshore of the natural
288 oyster reefs, and the offshore wave height was assumed to be the same as that for the oyster reef
289 living shoreline, as before. At all sites, the natural oyster reef was directly in line and adjacent to
290 the oyster reef living shoreline. There was, however, a significant difference in the wave heights
291 recorded between the offshore RBR for the control and oyster reef living shoreline treatments
292 ($t_{(122)} = -3.9571$, $P < 0.001$), although the mean \pm SE was similar for both treatments ($0.01 \pm$
293 0.001 m).

294

295 **Wave analysis**

296 The absolute pressure values recorded by the RBRs were converted to gauge pressure
297 using atmospheric pressure data obtained from the closest weather stations to each site
298 (Appendix S1: Fig. S1; Morris et al. 2019b). Wave data were post-processed to account for
299 shoaling and breaking, where appropriate, using the method detailed in Haynes (2018) and
300 (Morris et al. 2019b). Water densities were calculated using the Thermodynamic Equation of
301 Seawater – 2010 (TEOS-10; IOC et al. 2010), using the known salinity at each location and
302 water temperatures obtained from World Sea Temperatures (www.seatemperature.org). The
303 corrected pressure data were then converted to water depth using this calculated water density
304 (Eq. 1),

305
$$d = \frac{P}{\rho_w g} \quad (\text{Eq. 1})$$

306 where d is the water depth, P is the pressure, ρ_w is the density of water, and g is the acceleration
307 due to gravity.

308 The water levels were linearly detrended to remove low-frequency signal, which
309 provided an average water depth for each burst (of 1024 samples per hour, as above) and a zero-
310 average input for Fast-Fourier-Transform. A pressure response factor, K_p , was determined for
311 each frequency bin of the Fast-Fourier-Transform (Eq. 2; Kamphuis 2010),

312
$$K_p = \frac{\cosh(k(d+z))}{\cosh(kd)} \quad (\text{Eq. 2})$$

313 where k is the wave number, d is the water depth, and z is the logger level from the
314 surface. The wave energy density spectrum was then corrected for depth by dividing it by the
315 pressure response factor squared. The output wave energy density spectrum was divided into sea
316 (1 to 10 s period) and swell (10 to 20 s period) components (USACE 1984). Significant wave

317 heights for each logger (H_s ; using the zeroth-moment wave height) were determined from the
318 wave spectrum (Eq. 3; Moeller et al. 1996),

319
$$H_s = 4\sqrt{E_{total}/(\rho_w g)} \quad (\text{Eq. 3})$$

320 where E_{total} is the total energy defined as the integral of the wave energy density spectrum. The
321 wave period corresponding to the significant wave height, $T_{1/3}$, was approximated as $1.2 T_{m01}$,
322 where T_{m01} is the zero-crossing period (Eq. 4; Goda 2010),

323
$$T_{m01} = \sqrt{m_0/m_2} \quad (\text{Eq. 4})$$

324 where m_0 and m_2 are the zeroth and second moments of the wave energy density spectrum,
325 respectively. Linear wave theory was used to calculate wave length, celerity and group velocity,
326 based on wave conditions at the offshore logger and assuming wave period did not change as the
327 wave approached shore. Wave celerity at the onshore RBR within each treatment at a site was
328 estimated based on Hunt (1979). This was used to calculate the shoaling coefficient (Eq. 5;
329 Haynes 2018),

330
$$K_s = \sqrt{C_{g_off}/C_{g_on}} \quad (\text{Eq. 5})$$

331 where C_{g_off} is the offshore RBR wave group celerity, and C_{g_on} is the onshore RBR wave
332 group celerity. Predicted onshore wave heights were generated to account for shoaling (Eq. 6)
333 and breaking (using the co-efficient of 0.78 multiplied by the depth at the onshore gauge; Haynes
334 2018),

335
$$H_{s_pred} = H_{s_off} K_s \quad (\text{Eq. 6})$$

336 where H_{s_pred} is the predicted wave height and H_{s_off} is the offshore wave height. The wave
337 transmission coefficient was defined as the ratio of measured to predicted wave height (Eq. 7;
338 Haynes 2018), where the predicted wave height was the limiting of the shoaling or breaking
339 wave height,

340
$$K_t = H_{s_on}/H_{s_pred} \quad (\text{Eq. 7})$$

341 where H_{s_on} is the recorded wave height at the onshore RBR. The wave transmission coefficient
342 accounts for potential changes in wave height due to shoaling and breaking, but not other
343 processes that could not be controlled for in this study (e.g., refraction and diffraction). All
344 processing was done in MATLAB (MathWorks 1996) and resulted in hourly data for water
345 depth, significant wave height at each RBR, wave period and the wave transmission coefficient
346 during the period the RBRs were underwater (i.e. only at high tide for most locations).

347 The freeboard (m) was calculated as the reef height minus the water depth. The
348 inundation duration was calculated as the percentage of time the entire reef was submerged (i.e.,
349 the freeboard had a negative value) during the study period. The inundation period during the
350 study was compared to longer-term data using water levels at nearby USGS gauges (NOAA tides
351 and currents for Alabama; Appendix S1: Fig. S1). The difference between the reef crest elevation
352 and water level relative to NAVD88 was used to calculate the percentage of time the crest of the
353 reef was inundated. The reefs were categorised into more or less than 50% inundated; this
354 threshold was chosen as the lower limit of inundation for *C. virginica* (Table 1). Regression
355 slopes between onshore measured and predicted significant wave heights were compared for
356 controls, and oyster reefs based on inundation duration, width and construction material. Further
357 the wave heights were compared at controls, oyster reefs and either rock sills or natural oyster
358 reefs, at Virginia and Florida respectively. The effect of location (fixed, 3 levels: New Jersey,
359 Virginia, Florida), inundation duration (fixed, percentage), and age (fixed, years) on the
360 percentage cover of oysters was tested using a linear mixed effects model, with site nested in
361 location included as a random factor on log transformed data. A likelihood ratio test comparing

362 the model with and without site was used to obtain a p-value for this random effect. All analyses
363 were done in R 3.4.0 (R Core Team 2017).

364

365 **Results**

366 Significant wave heights recorded at the sites ranged from 0 – 0.35 m during the study period
367 (Fig. 2a). Average water depth between the gauge pairs ranged from 0.16 – 2.35 m (Fig. 2b),
368 after reef emersion time was truncated from each data set (i.e., low tide). The NJ2 site
369 experienced the greatest depth of inundation (freeboard = -1.88 m) due to a combination of the
370 low height of this reef and New Jersey experiencing the greatest tidal range (Table 2), with a
371 potential contribution of the greater wave heights recorded during the study period (Fig. 2a). The
372 LA1 and LA2 sites experienced the least inundation (freeboard = 0.86 m), with the crests
373 exposed 100% of the time (Table 2). The average freeboard of all reefs is listed in Appendix 1:
374 Table S1.

375 Three out of the 15 reefs had an inundation duration of less than 50% (FL1, LA1, LA2),
376 while the other 12 reefs were inundated more than 50% of the time and considered to be within
377 the tolerable aerial exposure limits for *C. virginica* (Table 1). Two reefs were fully inundated
378 during the study (AL1, AL2; Table 1, Fig. 2b). The categorisation of the reefs based on the
379 measured study conditions aligned with that estimated from the USGS gauges during the study
380 and longer-term from 2017-2019 (Table 1). In general, the inundation durations measured during
381 the study were representative of the longer-term data (Table 1), but at VA3 the inundation
382 duration was 30-40% greater during the study compared to the long-term data (Table 1). This is
383 likely due to the storm event captured causing wind and/or wave set-up, which generated the
384 second highest wave heights in the study (after NJ2; Fig. 2a). Similarly, the inundation duration

385 at FL3 was 20% less, and at AL3, 40% more during the study compared to the long-term data.

386 The reason for these differences is less clear but is likely due to the water level data from the
387 USGS gauges not being site specific, and therefore providing an estimation only.

388 There was little difference between the percent change in wave height between the
389 controls (5.9%) and oyster reefs that experienced greater than 50% inundation duration (4.5%);
390 Fig. 3a, b). In contrast, a 68.4% decrease in wave height was observed at reefs that were
391 inundated for less than 50% of the time (Fig. 3b). Despite this, when the freeboard was the same
392 between reefs that had either greater or less than 50% inundation duration, the wave attenuation
393 was also similar (Fig. 4). Wave transmission significantly decreased with increasing positive
394 freeboard and decreasing submergence for both inundation regimes (Fig. 4). Thus, the overall
395 result of a lower wave attenuation of reefs that have a greater inundation duration is driven by
396 these reefs experiencing less time at the optimal freeboard for wave attenuation (i.e., a reef crest
397 elevation that is either at or above the water level). Reefs that had an inundation duration of
398 greater than 50% were categorised based on the range of widths to determine if reefs of a greater
399 width had a lower wave transmission. Based on the range of reef widths observed in this study,
400 width had little effect on the wave transmission of these reefs (Fig. 3c). Whether the reefs were
401 made of shell or concrete also had less of an effect on wave transmission compared to reef height
402 (Fig. 3d).

403 On average, the rock sills were 2.5 times taller than the oyster reefs in Virginia and spent
404 35% or less time inundated during the study (Table 2). Rock sills reduced wave heights by 72%
405 compared to a 5% and 3% reduction in wave height at oyster reefs and controls, respectively
406 (Fig. 5a). In Florida, the restored oyster reefs were a similar width and height as the natural
407 unrestored reefs, with the latter having a slightly taller profile at FL2 and FL3 (Table 2). The

408 wave attenuation was greatest at the natural reefs (84%), followed closely by the restored oyster
409 reefs (75%), compared to the controls (35%; Fig. 5b). However, the percent of variance
410 explained by the linear model was lower at the natural (15%) and restored (31%) oyster reefs.

411 There was no significant effect of location ($F_{3,44}=0.03$, $P>0.05$), inundation duration
412 ($F_{1,4}=0.23$, $P>0.05$), or age ($F_{1,4}=0.01$, $P>0.05$) on the percentage cover of oysters. However,
413 there was a significant difference in the oyster cover among sites ($P<0.001$; Table 1).

414

415 **Discussion**

416 To achieve the goal of a sustainable coastal defence structure, oyster reef living shorelines must
417 be effective at both hazard risk reduction and habitat provisioning for oysters. Understanding the
418 coastal protection afforded by reefs within the habitat limitations of oysters is therefore
419 important for identifying the parametric ranges for which oyster reefs and coastal defence
420 overlap. Oyster reefs where the crest was inundated less than 50% of the time were almost 14
421 times more effective at reducing the wave heights observed during this study than those that had
422 an inundation duration of more than 50%. The width of the reefs that had > 50% inundation
423 ranged from 0.6 – 6.6 m; these widths had little effect on the wave transmission of the reefs.
424 Eight out of the nine study sites where oyster colonisation could be quantified experienced the
425 optimal inundation regime. However, the percentage cover of oysters varied among these sites,
426 with no effect of inundation duration, age, or location.

427 The duration and depth of inundation are determined by the intertidal elevation of the reef
428 and the tidal amplitude of an area (Byers et al. 2015), as well as periodic events such as storm-
429 driven wind or wave set-up. The duration and depth of inundation have an effect on wave
430 attenuation and on oyster recruitment, survival, and growth. Previous research has shown that

431 oyster reefs are very effective at attenuating waves when the reef crest height is at, or above, the
432 water level (Chauvin 2018, MacDonald 2018, Wiberg et al. 2018, Chowdhury et al. 2019, Zhu et
433 al. 2020, Spiering et al. in revision). This is because waves are strongly modified or break as they
434 cross the reef (Wiberg et al. 2018). As the water levels increase, a reduction in wave height is
435 instead caused by the interaction of oscillatory motion with the reef, the effect of which
436 decreases with increasing water depth (Wiberg et al. 2018). Here, our data support this finding,
437 showing that the negative relationship between wave transmission and reef submergence is
438 evident across the large biogeographic scale studied.

439 It has been noted previously that some of the reefs studied may only spend 10-25% of the
440 time at the optimal freeboard for wave attenuation (MacDonald 2018, Wiberg et al. 2018, Zhu et
441 al. 2020). When reefs become submerged, the wave attenuation can decrease to 0-20% (Wiberg
442 et al. 2018; Fig. 4). However, this inundation duration is within the optimal range for oyster
443 population establishment (Table 1). Critically, *C. virginica* do not tend to colonise substratum
444 where the inundation duration is less than approximately 50% (Ridge et al. 2015; Table 1). Reefs
445 with crests above this threshold will not be colonised by oysters, although if the reef base is
446 within the optimal range then oyster habitat may be provided lower on the structure, but this will
447 not result in an oyster reef that can build and maintain itself (i.e., wave attenuation is provided by
448 the artificial reef base not the growing oyster reef; Morris et al. 2019). Greater submergence
449 times enhance feeding, and therefore growth of oysters (Solomon et al. 2014), and reduce
450 desiccation stress. Too much immersion time, however, can negatively affect oysters due to
451 greater fouling or predation in the subtidal (Fodrie et al. 2014). Thus, there is an optimum
452 inundation duration that varies slightly along the geographical range, but seems to be within a 5-
453 40% range (Table 1). This translates to oyster reefs spending a greater percentage of time outside

454 of the freeboards that maximize wave attenuation, and can explain the overall difference in wave
455 attenuation of reefs that experienced more or less than 50% inundation duration in this study.

456 The extent to which the inundation duration affects wave attenuation is also dependent on
457 the tidal amplitude. Where the tidal range is low, the variation in wave attenuation will be less
458 than in areas that have a greater tidal range. Although all of the sites here are considered
459 microtidal (defined as a tidal range of 0–2 m as per Davies 1964), they still experienced a range
460 of tidal amplitudes (Table 2), with the reefs in New Jersey having a greater depth of inundation
461 than the other sites. In contrast to its effect on wave attenuation, an increased depth of inundation
462 can have a positive effect on oyster growth and reef height due to a greater volume of water
463 delivery per unit of time and flow velocity that affects feeding and larval delivery (Byers et al.
464 2015).

465 For the reefs where the percent cover of oysters could be measured, inundation duration
466 varied between 68-97% for all but one reef (FL1; 38%). This variation was similar to that found
467 across a 1,500 km region from North Carolina to Florida (52-84%; Byers et al. 2015), where
468 there was no effect of inundation duration across latitude, and therefore oyster reef properties.
469 There was, however, significant variation in percent cover of oysters among sites in this study
470 that was not a factor of inundation duration. Other physical variables that commonly affect
471 oyster reef properties are salinity and temperature (Byers et al. 2015). Temperature linearly
472 declines with increasing latitude, but as there was no effect of location on oyster cover, it is
473 unlikely to be the cause of the site variability. Similarly, given that oysters are found in each of
474 the areas studied, the salinity was considered to be suitable. Another factor that affects the
475 recruitment of reef substratum is larval availability. The reefs in this study relied on natural
476 recruitment from the water column. If the reefs are recruitment-limited then they may never

477 establish an oyster population; larval dispersal and connectivity are therefore important
478 considerations in the siting of reef substratum (Lipcius et al. 2008, Puckett et al. 2018). Further,
479 as coastal defences are inherently built in turbulent, wave exposed environments, an added
480 variable of the threshold of exposure for oyster reef establishment is critical in oyster reef living
481 shorelines (Whitman and Reidenbach, 2012). The benthic flow across the reef can be
482 manipulated to enhance larval recruitment by increasing topographic complexity that creates
483 interstitial spaces, which lower the shear stresses that can dislodge larvae (Whitman and
484 Reidenbach, 2012).

485 The comparison of rock sills to oyster reefs further supports the importance of crest
486 height for wave attenuation in narrow structures. Rock sills showed a similar magnitude of wave
487 height reduction as the oyster reefs that were exposed for more than 50% of the time, which
488 again was much greater than the oyster reefs in Virginia that all had <50% exposure. When
489 oyster reef living shorelines were compared to natural reefs in Florida, the wave attenuation was
490 similar between the two treatments (75% and 84%, respectively), and double that of the control
491 (35%). This is likely due to the similarity in size (height and width) of the restored and natural
492 reefs, as the restored reefs were deployed onto the historic footprint of natural degraded reefs.
493 However, the natural reefs had a very low percent cover of live oyster compared to the restored
494 reefs (except FL1). Live oysters increase bed roughness and therefore drag, which can lead to
495 better flow energy attenuation (Kitsikoudis et al. 2020). In contrast, degraded reefs consist of
496 loose disarticulated shells that can be moved around with wave events. Therefore, even though
497 the wave attenuation observed was similar between restored and natural degraded reefs here, it is
498 unclear how this may evolve through time, as degraded reefs could eventually disintegrate if not
499 colonised by oysters (Kitsikoudis et al. 2020). The pattern of wave attenuation across treatments

500 in Florida, when considered alone, was very different to the overall patterns observed, as greater
501 attenuation was recorded at both the control and oyster reefs, but it was also more variable. This
502 is likely due to Florida experiencing only very small wave heights for the duration of the
503 deployment. Smaller, high frequency waves (e.g., 1 s period) may have been under-sampled with
504 the 1 Hz frequency used to compare treatments in this study, which potentially resulted in the
505 reporting of smaller wave heights than were present. However, similar maximum wave heights
506 have been recorded at other sites in Mosquito Lagoon, Florida, using a 32 Hz sampling
507 frequency (Kibler et al. 2019), thus our results are just as likely to be due to the calm weather
508 during deployments and the fact that these sites are very sheltered under normal conditions.

509 At the other locations, there was a range in wave heights observed and these were
510 comparable to those in previous studies in New Jersey (average 0.03 - 0.11 m, maximum 0.15 -
511 0.55 m; MacDonald 2018), Virginia (average 0.03 - 0.10 m, maximum 0.30 - 0.50 m; Wiberg et
512 al. 2018) and Louisiana (average 0.10 m, maximum 0.45 m; Chauvin 2018). Nevertheless, these
513 wave heights were generally more representative of calm to average conditions due to the trade-
514 off between the large-scale of the study and wave sensor deployment duration (36 - 48 hours),
515 which limited the range of wave conditions that could be observed. The size of the waves
516 (Wiberg et al. 2018, Chowdhury et al. 2019), as well as whether they are swell- or wind-
517 dominated (Zhu et al. 2020) or accompanied by storm tides, impacts the efficacy of oyster reefs
518 at wave attenuation. Previous studies of oyster reefs have shown that for the equivalent water
519 depth, wave attenuation increases with wave height (Wiberg et al. 2018, Chowdhury et al. 2019).
520 This may explain why fringing oyster reefs have been found to have a greater impact on
521 shoreline retreat at higher exposure locations (La Peyre et al. 2015). Hence, there is the potential
522 that with larger wave heights the wave transmission values observed in this study could decrease

523 at oyster reef living shorelines. This highlights the need to examine multiple reefs experiencing
524 diverse conditions to get a complete understanding of how they work.

525 It is also important to consider the type of shoreline being protected, as habitat type can
526 influence susceptibility to erosion from different weather events. For example, saltmarsh was the
527 predominant shoreline type in our study. Leonardi et al. (2016) demonstrated that marsh-edge
528 erosion was caused by moderate, but high frequency (2.5 ± 0.5 per month) storms. Larger
529 storms, in contrast, are often accompanied by storm surge, which dissipates over the marsh bed
530 rather than impacting the marsh edge. Previous research on oyster reef living shorelines has
531 shown significant variability in erosion control of saltmarsh among sites (Meyer et al. 1997,
532 Piazza et al. 2005, Stricklin et al. 2010, Scyphers et al. 2011, La Peyre et al. 2013, Moody et al.
533 2013, La Peyre et al. 2014, 2015). Oyster reefs are likely to have the greatest effect on the
534 reduction of saltmarsh erosion when the elevation of the marsh platform coincides with the water
535 depths that maximize wave attenuation (i.e., when reef submergence is low; Wiberg et al. 2018).
536 As currently designed, reefs that are within the habitat requirements for oysters are likely to have
537 little effect on higher-elevation shorelines dominated by saltmarshes. How this process translates
538 to protection by oyster reefs for other shoreline habitat types is not well known.

539 Natural oyster reefs were once vast, with historical imagery suggesting reefs kilometres
540 long fringed the shorelines in the 1800s in Chesapeake Bay, Virginia (Woods et al. 2005). A
541 recent study in Mosquito Lagoon, Florida, found that small-scale restored oyster reefs (as studied
542 here) had a cumulative positive impact on erosion rates that may not be observed at a single site
543 (McClanahan et al. 2020). The variability in effectiveness of oyster reefs at providing erosion
544 control may be the result of a mismatch in the scale of the construction of living shorelines and
545 that required for delivery of the coastal defence service. For example, McClanahan et al. (2020)

546 demonstrated that the combined 89 smaller oyster reef projects had a landscape scale effect
547 within this ecosystem. At an individual scale, the reefs we studied were narrow structures. The
548 range of widths observed had little effect on the wave attenuation of the reefs that were at the
549 appropriate elevation for oysters. However, physical modelling of submerged rubble-mound
550 breakwaters (Seabrook and Hall, 1998) and bagged oyster shell reefs (Allen and Webb, 2011)
551 showed that wider structures of the same elevation can further decrease wave transmission by
552 20-40%. Field studies have shown width to be important for wave attenuation in saltmarshes
553 (Shepard et al. 2011) and coral reefs (Ferrario et al. 2014), however, this factor has not been
554 examined for oyster reefs. This is likely due to most of our knowledge on the wave transmission
555 of oyster reefs being generated from studies on living shorelines, with a paucity of information
556 available on natural reefs (Narayan et al. 2016). For living shorelines to be used as a tool for
557 restoration and risk reduction, it is imperative that we optimize the design to maximize both
558 ecological and engineering outcomes.

559

560 **Conclusions**

561 In the face of a changing climate, there is an increasing interest in living shorelines as an
562 adaptive and sustainable coastal defence strategy. For living shorelines to be successful, they
563 need to establish a self-sustaining population of the target species and have the ability to provide
564 coastal protection under the conditions that cause erosion and/or flooding. This large-scale study
565 across multiple states provides a broader perspective on the diversity of oyster reef living
566 shoreline approaches. We showed that many of the living shoreline approaches using oysters
567 failed to optimize the ecological and engineering goals. To date, studies have focused on
568 understanding the wave attenuation of oyster reefs without integrating consideration for the

569 ecological limitations of oysters. This has resulted in a focus on how the crest of the reef
570 influences wave transmission. However, given that this design parameter needs to stay within the
571 optimal inundation duration for oysters, efforts should be refocused to understand the effects of
572 other design parameters, such as reef width, on maximising wave attenuation over a greater
573 inundation range. This approach should apply generally to the design and implementation of
574 living shorelines, where the engineering parameters are calculated to account for the ecological
575 limitations of a species in order to achieve both goals. Identifying the circumstances under which
576 living shorelines can be designed to achieve these goals is also important to determine the
577 thresholds for their use successfully. Our results suggest that the low-crested, narrow oyster reefs
578 that are commonly built are, on average, not effective at wave attenuation. Their ability to
579 provide erosion control, however, will also depend on the elevation of the shoreline and the
580 conditions that contribute to local erosion. This combination of factors has likely contributed to
581 the large variation in erosion control by oyster reef living shorelines reported in the literature. A
582 broader understanding of the reef characteristics and seascape contexts that result in effective
583 coastal defence by oyster reefs is needed to inform the design of future living shoreline projects.
584 This continued research effort will ensure that oyster reef living shorelines are successful in
585 achieving both their ecological and engineering goals.

586

587 **Acknowledgements**

588 We thank T. Graham for his advice on data processing and J. Shinn for her assistance with the
589 New Jersey sites. R.L.M. was supported by an Early Career Researcher Global Mobility Grant
590 from The University of Melbourne. The National Centre for Coasts and Climate is funded
591 through the Earth Systems and Climate Change Hub by the Australian Government's National

592 Environmental Science Program. This paper is Contribution No. 3990 of the Virginia Institute of
593 Marine Science, William & Mary. Any use of trade, firm, or product names is for descriptive
594 purposes only and does not imply endorsement by the U.S. Government.

595

596 **References**

597 Allen, R. J., and B. M. Webb. 2011. Determination of wave transmission coefficients for oyster
598 shell bag breakwaters. *Coastal Engineering Practice*:684-697.

599 Beck, M. W., R. D. Brumbaugh, L. Aioldi, A. Carranza, L. D. Coen, C. Crawford, O. Defeo, G.
600 J. Edgar, B. Hancock, M. C. Kay, H. S. Lenihan, M. W. Luckenbach, C. L. Toropova, G.
601 F. Zhang, and X. M. Guo. 2011. Oyster reefs at risk and recommendations for
602 conservation, restoration, and management. *Bioscience* 61:107-116.

603 Bilkovic, D. M., M. Mitchell, P. Mason, and K. Duhring. 2016. The role of living shorelines as
604 estuarine habitat conservation strategies. *Coastal Management* 44:161-174.

605 Bulleri, F., and M. G. Chapman. 2010. The introduction of coastal infrastructure as a driver of
606 change in marine environments. *Journal of Applied Ecology* 47:26-35.

607 Byers, J. E., J. H. Grabowski, M. F. Piehler, A. R. Hughes, H. W. Weiskel, J. C. Malek, and D.
608 L. Kimbro. 2015. Geographic variation in intertidal oyster reef properties and the
609 influence of tidal prism. *Limnology and Oceanography* 60:1051-1063.

610 Carter, J., C. Connor, J. Todd, A. Agarwal, and H. Bermudez. 2016. Living shoreline
611 demonstration project, prepared for Louisiana Coastal Protection and Restoration
612 Authority. Coast and Harbor Engineering, a division of Mott MacDonald, New Orleans.

613 Casas, S. M., J. La Peyre, and M. K. La Peyre. 2015. Restoration of oyster reefs in an estuarine
614 lake: population dynamics and shell accretion. *Marine Ecology Progress Series* 524:171-
615 184.

616 Chauvin, J. M. 2018. Wave attenuation by constructed oyster reef breakwaters. Louisiana State
617 University, Louisiana, US.

618 Chowdhury, M. S. N., B. Walles, S. M. Sharifuzzaman, M. Shahadat Hossain, T. Ysebaert, and
619 A. C. Smaal. 2019. Oyster breakwater reefs promote adjacent mudflat stability and salt
620 marsh growth in a monsoon dominated subtropical coast. *Scientific Reports* 9:8549.

621 Coast and Harbor Engineering, CHE. 2014. Living Shoreline Demonstration Project, Coastal
622 Engineering and Alternatives Analysis. Baton Rouge, LA. October 9, 2014.

623 Coen, L. D., and A. T. Humphries. 2017. Chapter 19. Oyster-generated marine habitats: their
624 services, enhancement and monitoring. In: S. Stuart and S. Murphy (eds) Routledge
625 Handbook of Ecological and Environmental Restoration, Routledge: New York, 274-
626 294.

627 Colvin, J., S. Lazarus, M. Splitt, R. Weaver, and P. Taeb. 2018. Wind driven setup in
628 east central Florida's Indian River Lagoon: forcings and parameterizations. *Estuarine,
Coastal and Shelf Science* 213:40-48.

629 Coghlan, I. R., Howe, D. and W. C. Glamore. 2016. Preliminary testing of oyster shell filled
630 bags. WRL Technical Report 2015/20, January.

631 Davies, J. L. 1964. A morphogenic approach to world shorelines. *Zeitschrift Fur
632 Geomorphologie* 8:27-42.

633 Ferrario, F., M. W. Beck, C. D. Storlazzi, F. Micheli, C. C. Shepard, and L. Airoldi. 2014. The
634 effectiveness of coral reefs for coastal hazard risk reduction and adaptation. *Nature
635 Communications* 5:3794.

636 Fodrie, F. J., A. B. Rodriguez, C. J. Baillie, M. C. Brodeur, S. E. Coleman, R. K. Gittman, D. A.
637 Keller, M. D. Kenworthy, A. K. Poray, J. T. Ridge, E. J. Theuerkauf, and N. L. Lindquist.
638 2014. Classic paradigms in a novel environment: inserting food web and productivity

639 lessons from rocky shores and saltmarshes into biogenic reef restoration. *Journal of*
640 *Applied Ecology* 51:1314-1325.

641 Garvis, S. K. 2009. Quantifying the impacts of oyster reef restoration on oyster coverage, wave
642 dissipation and seagrass recruitment in Mosquito Lagoon, Florida. University of Central
643 Florida, Florida, United States.

644 Goda, Y. 2010. Random seas and design of maritime structures. World Scientific Publishing Co.
645 Pte. Ltd., Singapore.

646 Grabowski, J. H., R. D. Brumbaugh, R. F. Conrad, A. G. Keeler, J. J. Opaluch, C. H. Peterson,
647 M. F. Piehler, S. P. Powers, and A. R. Smyth. 2012. Economic valuation of ecosystem
648 services provided by oyster reefs. *Bioscience* 62:900-909.

649 Haynes, K. M. 2018. Field measurements of boat wake attenuation in coastal salt marshes.
650 University of South Alabama.

651 Heck, K., J. Cebrian, S. Powers, R. Gericke, C. Pabody, and J. Goff. 2012. Final Monitoring
652 Report to the Nature Conservancy: Coastal Alabama Economic Recovery and Ecological
653 Restoration Project: Creating jobs to protect shorelines, restore oyster reefs and enhance
654 fisheries productions, Dauphin Island Sea Lab and University of South Alabama,
655 Dauphin Island.

656 Hernandez, A. B., R. D. Brumbaugh, P. Frederick, R. Grizzle, M. W. Luckenbach, C. H.
657 Peterson, and C. Angelini. 2018. Restoring the eastern oyster: how much progress has
658 been made in 53 years? *Frontiers in Ecology and the Environment* 16:1-9.

659 Hinkel, J., D. Lincke, A. T. Vafeidis, M. Perrette, R. J. Nicholls, R. S. J. Tol, B. Marzeion, X.
660 Fettweis, C. Ionescu, and A. Levermann. 2014. Coastal flood damage and adaptation

661 costs under 21st century sea-level rise. *Proceedings of the National Academy of Sciences*
662 111:3292-3297.

663 Hunt, J. N. 1979. Direct solution of wave dispersion equation. *Journal of Waterway, Port,*
664 *Coastal, and Ocean Engineering* 4:457-459.

665 IOC, SCOR, and IAPSO. 2010. The international thermodynamic equation of seawater – 2010:
666 calculation and use of thermodynamic properties. *Intergovernmental Oceanographic*
667 *Commission, Manuals and Guides No. 56, UNESCO.*

668 Kamphuis, J. W. 2010. Introduction to coastal engineering and management, Advanced series on
669 ocean engineering. *World Scientific, Singapore.*

670 Kibler, K. M., V. Kitsikoudis, M. Donnelly, D. W. Spiering, and L. Walters. 2019. Flow–
671 vegetation interaction in a living shoreline restoration and potential effect to mangrove
672 recruitment. *Sustainability* 11:3215.

673 Kitskoudis, V., K. M. Kibler, and L. J. Walters. 2020. In-situ measurements of turbulent flow
674 over intertidal natural and degraded oyster reefs in an estuarine lagoon. *Ecological*
675 *Engineering* 143:1056882.

676 Kohler, K. E., and S. M. Gill. 2006. Coral Point Count with Excel extensions (CPCe): A Visual
677 Basic program for the determination of coral and substrate coverage using random point
678 count methodology. *Computers and Geosciences* 32:1259-1269.

679 La Peyre, M. K., A. T. Humphries, S. M. Casas, and J. F. La Peyre. 2014. Temporal variation in
680 development of ecosystem services from oyster reef restoration. *Ecological Engineering*
681 63:34-44.

682 La Peyre, M. K., L. Schwarting, and S. Miller. 2013. Preliminary assessment of bioengineered
683 fringing shoreline reefs in Grand Isle and Breton Sound, Louisiana. Report 2013-1040,
684 Reston, VA.

685 La Peyre, M. K., K. Serra, T. A. Joyner, and A. Humphries. 2015. Assessing shoreline exposure
686 and oyster habitat suitability maximizes potential success for sustainable shoreline
687 protection using restored oyster reefs. *PeerJ*, 3, e1317.

688 Leonardi, N., N. K. Ganju, and S. Fagherazzi. 2016. A linear relationship between wave power
689 and erosion determines salt-marsh resilience to violent storms and hurricanes.
690 *Proceedings of the National Academy of Sciences* 113:64.

691 Lipcius, R. N., D. B. Eggleston, S. J. Schreiber, R. D. Seitz, J. Shen, M. Sisson, W. T.
692 Stockhausen, and H. V. Wang. 2008. Importance of metapopulation connectivity to
693 restocking and restoration of marine species. *Reviews in Fisheries Science* 16:101-110.

694 Livingston, R. J., R. L. Howell, X. F. Niu, F. G. Lewis, and G. C. Woodsum. 1999. Recovery of
695 oyster reefs (*Crassostrea virginica*) in a gulf estuary following disturbance by two
696 hurricanes. *Bulletin of Marine Science* 64:465-483.

697 MacDonald, M. 2018. Wave monitoring and sedimentation analysis at four oyster castle
698 breakwaters at Gandy's Beach, NJ. For: The Nature Conservancy. New Jersey, US.

699 Manis, J. E., S. K. Garvis, S. M. Jachec, and L. J. Walters. 2015. Wave attenuation experiments
700 over living shorelines over time: a wave tank study to assess recreational boating
701 pressures. *Journal of Coastal Conservation* 19:1-11.

702 Marshall, D. A. and La Peyre, M. K. 2020. Effects of inundation duration on southeastern
703 Louisiana oyster reefs. *Experimental Results*.

704 MathWorks, I. 1996. MATLAB : the language of technical computing : computation,
705 visualization, programming : installation guide for UNIX version 5. Natwick: Math
706 Works Inc., 1996.

707 McClenachan, G. M., M. J. Donnelly, M. N. Schaffer, P. E. Sacks, and L. J. Walters. 2020. Does
708 size matter?: Quantifying the cumulative impact of small-scale living shoreline and
709 oyster reef restoration projects on shoreline erosion. *Restoration Ecology*
710 <https://doi.org/10.1111/rec.13235>.

711 Meucci, A., I. R. Young, M. Hemer, E. Kirezci, and R. Ranasinghe. 2020. Projected 21st century
712 changes in extreme wind-wave events. *Science Advances* 6:eaaz7295.

713 Meyer, D. L., E. C. Townsend, and G. W. Thayer. 1997. Stabilization and erosion control value
714 of oyster cultch for intertidal marsh. *Restoration Ecology* 5:93-99.

715 Mitchell, M., and D. M. Bilkovic. 2019. Embracing dynamic design for climate-resilient living
716 shorelines. *Journal of Applied Ecology* Doi: 10.1111/1365-2664.13371.

717 Moeller, I., T. Spencert, and J. R. French. 1996. Wind wave attenuation over saltmarsh surfaces:
718 preliminary results from Norfolk, England. *Journal of Coastal Research* 12:1009-1016.

719 Moody, J., D. Kreeger, S. Bouboulis, S. Roberts, and A. Padeletti. 2016. Design,
720 implementation, and evaluation of three living shoreline treatments at the DuPont Nature
721 Center, Mispillion River, Milford, DE., Partnership for the Delaware Estuary,
722 Wilmington.

723 Moody, R. M., J. Cebrian, S. M. Kerner, K. L. Heck, S. P. Powers, and C. Ferraro. 2013. Effects
724 of shoreline erosion on salt-marsh floral zonation. *Marine Ecology Progress Series*
725 488:145-155.

726 Morris, R. L., D. M. Bilkovic, M. K. Boswell, D. Bushek, J. Cebrian, J. Goff, K. M. Kibler, M.
727 K. La Peyre, G. McClenachan, J. Moody, P. Sacks, J. P. Shinn, E. L. Sparks, N. A.
728 Temple, L. J. Walters, B. M. Webb, and S. E. Swearer. 2019a. The application of oyster
729 reefs in shoreline protection: are we over-engineering for an ecosystem engineer? *Journal*
730 of Applied Ecology Doi: 10.1111/1365-2664.13390.

731 Morris, R. L., A. Boxshall, and S. E. Swearer. 2020. Climate-resilient coasts require diverse
732 defence solutions. *Nature Climate Change* 10:485-487.

733 Morris, R. L., T. D. J. Graham, J. Kelvin, M. Ghisalberti, and S. E. Swearer. 2019b. Kelp beds as
734 coastal protection: wave attenuation of *Ecklonia radiata* in a shallow coastal bay *Annals*
735 of Botany Doi: 10.1093/aob/mcz127.

736 Narayan, S., M. W. Beck, B. G. Reguero, I. J. Losada, B. van Wesenbeeck, N. Pontee, J. N.
737 Sanchirico, J. C. Ingram, G. M. Lange, and K. A. Burks-Copes. 2016. The effectiveness.
738 costs and coastal protection benefits of natural and nature-based defences. *PLoS ONE* 11.

739 Neumann, B., A. T. Vafeidis, J. Zimmermann, and R. J. Nicholls. 2015. Future coastal
740 population growth and exposure to sea-level rise and coastal flooding - A global
741 assessment. *PLoS ONE* 10:e0118571.

742 Piazza, B. P., P. D. Banks, and M. K. La Peyre. 2005. The potential for created oyster shell reefs
743 as a sustainable shoreline protection strategy in Louisiana. *Restoration Ecology* 13:499-
744 506.

745 Puckett, B. J., S. J. Theuerkauf, D. B. Eggleston, R. Guajardo, C. Hardy, J. Gao, and R. A.
746 Luettich. 2018. Integrating Larval Dispersal, Permitting, and Logistical Factors Within a
747 Validated Habitat Suitability Index for Oyster Restoration. *Frontiers in Marine Science*
748 5:75.

749 R Core Team. 2017. R: A Language and Environment for Statistical Computing. R Foundation
750 for Statistical Computing, Vienna Austria. Available online at : <http://www.R-project.org>

751 Ridge, J. T., A. B. Rodriguez, F. J. Fodrie, N. L. Lindquist, M. C. Brodeur, S. E. Coleman, J. H.
752 Grabowski, and E. J. Theuerkauf. 2015. Maximizing oyster-reef growth supports green
753 infrastructure with accelerating sea-level rise. *Scientific Reports* 5:14785.

754 Ridge, J. T., A. B. Rodriguez, and F. J. Fodrie. 2017. Salt Marsh and Fringing Oyster Reef
755 Transgression in a Shallow Temperate Estuary: Implications for Restoration,
756 Conservation and Blue Carbon. *Estuaries and Coasts* 40:1013-1027.

757 Rodriguez, A. B., F. J. Fodrie, J. T. Ridge, N. L. Lindquist, E. J. Theuerkauf, S. E. Coleman, J.
758 H. Grabowski, M. C. Brodeur, R. K. Gittman, D. A. Keller, and M. D. Kenworthy. 2014.
759 Oyster reefs can outpace sea-level rise. *Nature Climate Change* 4:493-497.

760 Salvador de Paiva, J. N., B. Walles, T. Ysebaert, and T. J. Bouma. 2018. Understanding the
761 conditionality of ecosystem services: the effect of tidal flat morphology and oyster reef
762 characteristics on sediment stabilization by oyster reefs. *Ecological Engineering* 112:89-
763 95.

764 Scyphers, S. B., S. P. Powers, K. L. Heck, and D. Byron. 2011. Oyster reefs as natural
765 breakwaters mitigate shoreline loss and facilitate fisheries. *PLoS ONE* 6:e22396.

766 Seabrook, S. and K. Hall. 1998. Wave transmission at submerged rubblemound breakwaters.
767 *Coastal Engineering Proceedings* 1 (26).

768 Seers, B. 2018. *fetchR*: calculate wind fetch.

769 Sharma, S., J. Goff, R. M. Moody, A. McDonald, D. Byron, K. L. Heck, Jr., S. P. Powers, C.
770 Ferraro, and J. Cebrian. 2016. Effects of shoreline dynamics on saltmarsh vegetation.
771 *PLoS ONE* 11:e0159814.

772 Shepard, C. C., C. M. Crain, and M. W. Beck. 2011. The protective role of coastal marshes: a
773 systematic review and meta-analysis. PLoS ONE 6:e27374.

774 Solomon, J. A., M. J. Donnelly, and L. J. Walterst. 2014. Effects of sea level rise on the intertidal
775 oyster *Crassostrea Virginica* by field experiments. Journal of Coastal Research 68:57-64.

776 Spiering, D. W., K. M. Kibler, V. Kitskoudis, M. Donnelly, and L. J. Walters. in revision.
777 Detecting hydrodynamic changes after living shoreline restoration and through an
778 extreme event using a Before-After-Control-Impact experiment. Estuaries and Coasts.

779 Stricklin, A. G., M. S. Peterson, J. D. Lopez, C. A. May, and C. F. Mohrman. 2010. Do small,
780 patchy, constructed intertidal oyster reefs reduce salt marsh erosion as well as natural
781 reefs? Gulf and Caribbean Research 22:21-27.

782 Styles, R. 2015. Flow and turbulence over an oyster reef. Journal of Coastal Research 31:978-
783 985.

784 The Nature Conservancy. 2017. Gandy's Beach shoreline protection project - final performance
785 report. The Nature Conservancy, Delmont.

786 USACE. 1984. Shore protection manual. U.S. Army Corps of Engineers, Mississippi.

787 van der Meer, J. W., R. Briganti, B. Zanuttigh, and B. Wang. 2005. Wave transmission and
788 reflection at low-crested structures: design formulae, oblique wave attack and spectral
789 change. Coastal Engineering 52:915-929.

790 Webb, B. M., and R. J. Allen. 2015. Wave transmission through artificial reef breakwaters.
791 Coastal Structures and Solutions to Coastal Disasters. ASCE.

792 Whitman, E. R., and M. A. Reidenbach. 2012. Benthic flow environments affect recruitment of
793 *Crassostrea virginica* larvae to an intertidal oyster reef. Marine Ecology Progress Series
794 463:177-191.

795 Wiberg, P. L., S. R. Taube, A. E. Ferguson, M. R. Kremer, and M. A. Reidenbach. 2018. Wave
796 attenuation by oyster reefs in shallow coastal bays. *Estuaries and Coasts* 42:331–347.

797 Woods, H., W. J. Hargis, C. H. Hershner, and P. A. M. Mason. 2005. Disappearance of the
798 natural emergent 3-dimensional oyster reef system of the James River, Virginia 1871-
799 1948. *Journal of Shellfish Research* 24:139-142.

800 Wright, L. D., R. A. Gammisch, and R. J. Byrne. 1990. Hydraulic roughness and mobility of
801 three oyster-bed artificial substrate materials. *Journal of Coastal Research* 6:867-878.

802 Young, I. R., S. Zieger, and A. V. Babanin. 2011. Global trends in wind speed and wave height.
803 *Science* 332:451.

804 Zhu, L., Q. Chen, H. Wang, W. Capurso, L. Niemoczynski, K. Hu, and G. Snedden. 2020. Field
805 Observations of Wind Waves in Upper Delaware Bay with Living Shorelines. *Estuaries and Coasts* 43:739-755.

807

808

809

810

811

812

813

814

815

816

817

818

819

820 Table 1. Studies that have reported the percent of time a reef should be inundated for the optimal
821 recruitment, survival and/or growth of *Crassostrea virginica*.

State	Inundation duration
North Carolina	82 – 95% ¹
North Carolina	60 – 80 % ²
North Carolina	72 – 82 % ³
North Carolina to Florida	52 – 84% ⁴
Florida	80 – 95% ⁵
Louisiana	52 – 94% ⁶

¹Fodrie et al. (2014); ²Ridge et al. (2014); ³Ridge et al.

(2017); ⁴Byers et al. (2015); ⁵Solomon et al. (2014);

⁶Marshall and La Peyre (2020)

822

823

824

825

826

827

828

829

830

831

832

833

834

835

836

837

838

839

840

841

842 Table 2. Characteristics of oyster reef living shorelines and rock sills and natural oyster reefs.
 843 Crest elevation where available is given in metres relative to NAVD88. Age is number of years
 844 at time of study. The percent of time the structures are inundated (% inundation duration) is
 845 given when (a) measured during RBR deployment; (b) calculated based on USGS gauges for
 846 deployment period; and (c) calculated based on USGS gauges from January 2017 – August 2019.
 847 For more oyster reef living shorelines characteristics refer to Appendix 1: Table S1. *Note this
 848 site is in Delaware. - data unavailable.

State/ Reef	Type	Age (yrs)	Length × Width (m)	Height (m)	Crest elevation	Tidal range (m)	% inundation duration			% oysters (±SE)
							(a)	(b)	(c)	
NJ1	Concrete	2	6 × 1	0.65	-0.48		82.4	87.7	80.2	41.2 ± 5.2
NJ2	Shell	2	51 × 6	0.17	-0.57	1.7	68.7	74.7	75.2	0.4 ± 0.4
NJ3*	Concrete	4	2 × 1	0.53	0.01		68.7	58.6	52.6	11.3 ± 4.4
VA1	Concrete	2	16 × 0.6	0.40	0.00		67.6	53.4	50.9	6.2 ± 1.7
VA2	Shell	1	35 × 0.9	0.30	0.04	0.7	75.7	66.1	54.4	0
VA3	Concrete	1	28 × 0.85	0.30	0.01		90.9	80.0	53.5	0
FL1	Shell	8	55 × 5.25	0.64	-		38.1	-	-	2.4 ± 1.6
FL2	Shell	1	30 × 6.67	0.29	0.41	0.3	97.2	100	98	74.0 ± 3.5
FL3	Shell	2	20 × 4	0.27	0.38		75.6	100	98	34.4 ± 6.1
AL1	Shell	9	65 × 5	0.60	-0.37		100	100	99.4	-
AL2	Concrete	8	125 × 2.28	0.23	-0.24	0.4	100	100	98.3	-
AL3	Shell	8	125 × 2.64	0.31	0.17		92.9	66.7	50.4	-
LA1	Concrete	1.5	130 × 2.7	1.40	0.84		0	0	1.2	-
LA2	Concrete	1.5	178 × 5.5	1.40	0.66	0.4	0	0	4.8	-
LA3	Concrete	7	75 × 3	1.10	-0.06		63.0	81.0	84.4	-
VA1	Rock sill	2	29.4 × 2.4	0.69	0.46		30.7	8.9	9.2	1.2 ± 0.4
VA2	Rock sill	7	41.3 × 1.9	0.84	0.40	0.7	35.7	16.3	13.9	14.4 ± 4.5
VA3	Rock sill	1	51.4 × 3.6	1.02	1.03		8.9	0	0.02	0
FL1	Natural	-	47 × 7.8	0.64	-		38.1	-	-	0.4 ± 0.4

FL2	Natural	-	35 × 5.9	0.49	-	0.3	58.3	-	-	4.0 ± 2.7
FL3	Natural	-	35 × 3.1	0.33	-		64.4	-	-	2.4 ± 1.7

849

850

851

852

853

854

855

856

857

858

859

860

861

862

863

864

865

866

867

868

869

870

871

872

873

874

875 Figure 1. A map of the five study areas. In each study area (red dots) there were three oyster
876 reef-control pairs, a schematic example of the wave logger (RBR) set-up for one pair is shown.
877 The circles (oyster reef treatment) and triangles (control treatment; no reef) indicate wave sensor
878 deployment (not to scale). For a detailed map of each area see Appendix 1: Fig. S1.

879 Figure 2. (a) Significant wave heights (m) at the offshore wave logger (RBR); and (b) the
880 average depth (m) recorded during each burst at 15 oyster reef living shorelines across five
881 locations (New Jersey/Delaware, Virginia, Florida, Alabama, Louisiana from left to right). The
882 red lines in (b) indicate the height of the reef (m; matching scale on y-axis).

883 Figure 3. Comparisons of measured (y-axis) and predicted (x-axis) significant wave height (m)
884 for (a) control ($R^2=0.97$); (b) oyster reef living shorelines with an inundation duration above 50%
885 ($R^2=0.97$) and below 50% ($R^2=0.78$); (c) reefs that have an inundation duration of more than
886 50% and widths of less than 1 m ($R^2=0.97$), 2-4 m ($R^2=0.97$) and 5-7 m ($R^2=0.96$); and (d) reefs
887 constructed of concrete ($R^2=0.88$) and shell ($R^2=0.96$). Values below the dotted line indicate a
888 decrease in wave height. The decrease in wave height is given as a percentage on the graphs. The
889 shaded area is the 95% confidence interval.

890 Figure 4. Correlation between the wave transmission coefficient (K_t) and freeboard (m) for reefs
891 that have an inundation duration of less or greater than 50%. A wave transmission value of less
892 than one indicates a reduction in wave height. A positive or negative freeboard value indicates
893 the reef is emerged or submerged, respectively. The shaded area is the 95% confidence interval.

894 Figure 5. Comparisons of measured (y-axis) and predicted (x-axis) significant wave height (m)
895 for (a) control ($R^2=0.99$), rock sill ($R^2=0.94$), and oyster reef living shoreline ($R^2=0.98$) in
896 Virginia; (b) control ($R^2=0.84$), natural oyster reef ($R^2=0.15$), and oyster reef living shoreline

897 (R²=0.31) in Florida. Values below the dotted line indicate a decrease in wave height. The
898 shaded area is the 95% confidence interval.

899

900

901

902

903

904

905

906

907

908

909

910

911

912

913

914

915

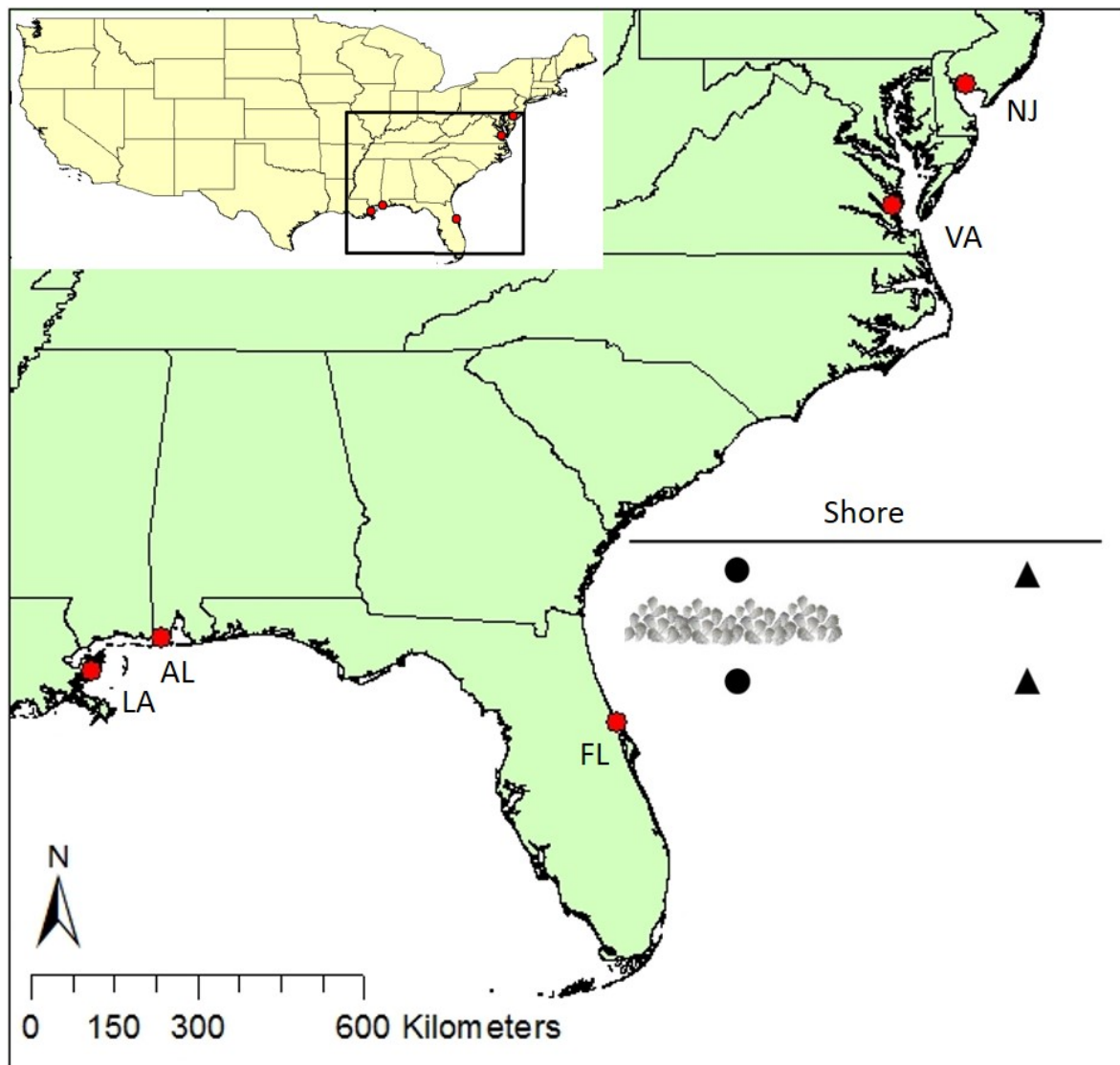
916

917

918

919

920 Figure 1



921

922

923

924

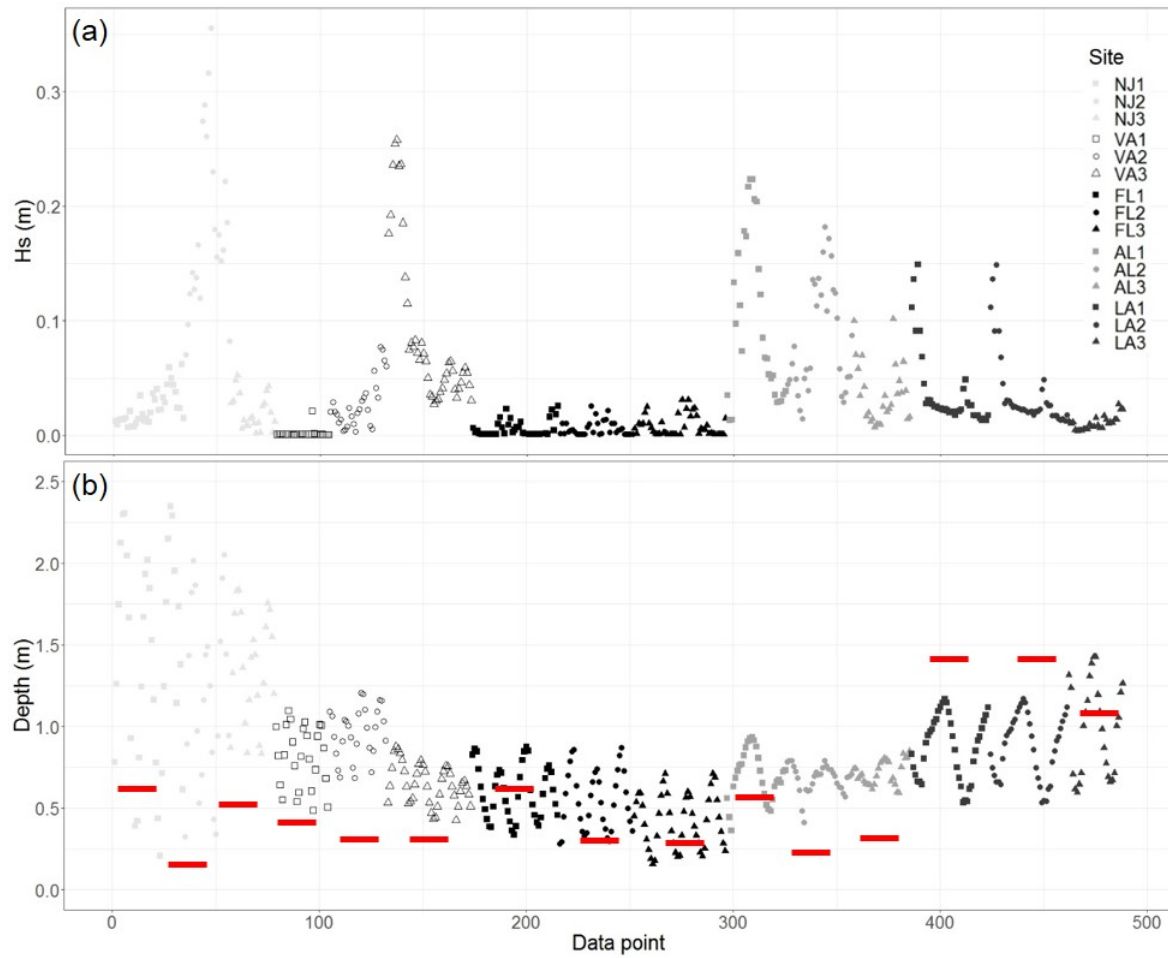
925

926

927

928

929 Figure 2



930

931

932

933

934

935

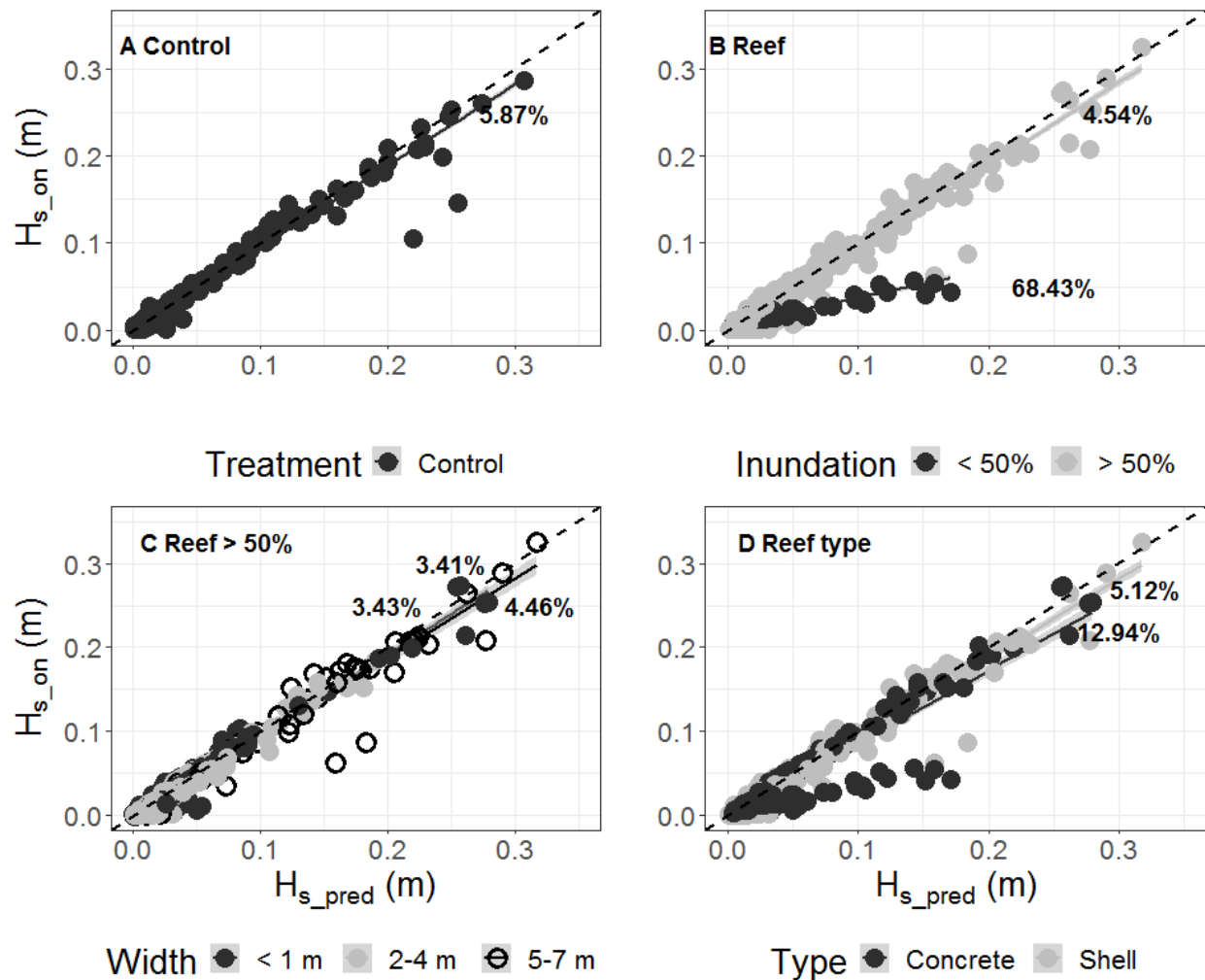
936

937

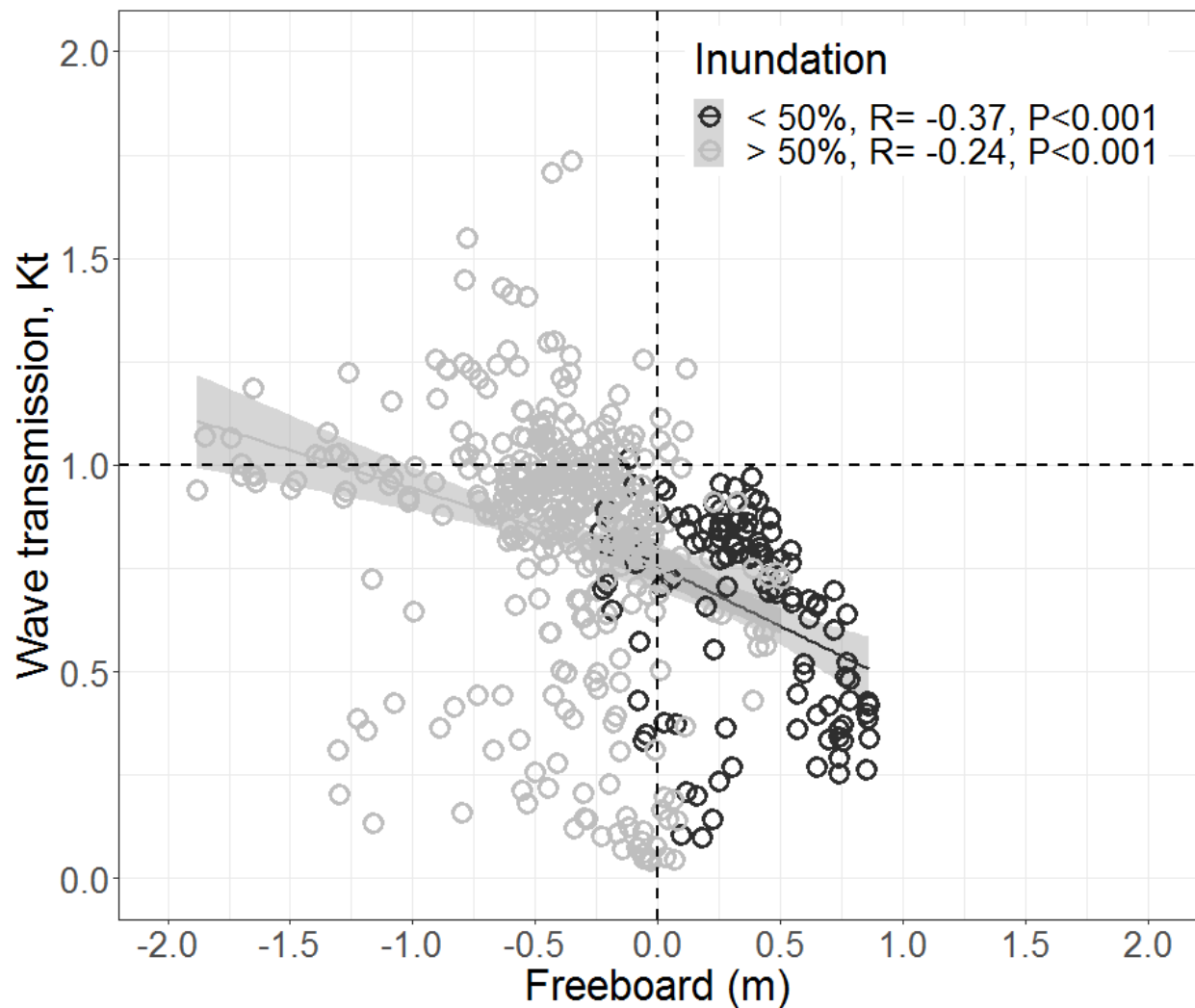
938

939

940 Figure 3



950 Figure 4



960 Figure 5

